

One-dimensional study of a Bifacial Silicon Solar Cell Illuminated from the Front Surface by a Monochromatic Light Under Frequency Modulation: Influence of Irradiation and Damage Coefficient

¹Mouhamadou Mously Diallo, ⁴Boureima Seibou, ²Hamet Yoro BA, ³Issa Zerbo, ¹Gregoire SISSOKO
 (gsissoko@yahoo.com)

¹Laboratory of Semiconductors and Solar Energy, Physics Department, Faculty of Science and Technology
 University Cheikh Anta Diop – Dakar – SENEGAL.

²Electromechanical Engineering Department, Polytechnic School of Thies – SENEGAL.

³Laboratory of Thermal and renewable energies - Ouagadougou University.

Abstract - In this article, a theoretical study based on some electrical parameters and intrinsic recombination velocities of a solar cell in frequency modulation and under irradiation, is presented. From the continuity equation, the density of the photo generated minority carriers in the base, the photocurrent and the phototension are determined in term of the angular frequency, of the damage coefficient and the irradiation energy. By means of Bode and Nyquist diagrams of the recombination velocities at the junction S_f and at the rear side S_b of the solar cell, equivalent electric model is proposed.

Key Words - Irradiation - damage Coefficient- frequency Modulation –Bode Diagram - Nyquist Diagram.

1. INTRODUCTION

The sun give off permanently electromagnetic radiations along with particles or corpuscles from the solar wind. It's essentially about electrons and positive ions (cations). The radiations of these charged and highly energy particles can modify the phenomenological and macroscopic parameters of the solar cells. In fact, when there is absorption of ionizing particles, the concentration in pair electron-hole within the cell is modified and the solar cell parameters are strongly modified.

This article is about a 1D theoretical study of a bifacial silicon solar cell illuminated by its front side, with a monochromatic light in frequency modulation. We will study the effect of the irradiation and the damage coefficient on some parameters of the cell, and finally from the Bode and Nyquist representations of the intrinsic recombination velocities of the solar cell, an equivalent electric model is proposed.

2. THEORETICAL STUDY

Let's consider an n+-p-p+ [1; 2] type of a polycrystalline silicon solar cell with back surface field (BSF) whose structure is schematized on figure1:

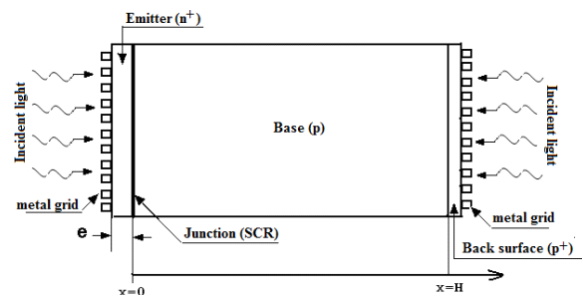


Figure 1: An n+-p-p+ structure of a silicon solar cell.

In the following study, the contribution of the emitter and the crystalline field that exists within the base are neglected. When the solar cell is illuminated front the front surface in frequency modulation, the excess minority carriers generated in the base explaining the different phenomena taken place in it is given by the equation (1), with the origin of the axis taken at the junction:

$$\frac{\partial^2 \delta(x,t)}{\partial x^2} - \frac{1}{D} \frac{\partial \delta(x,t)}{\partial t} - \frac{\delta(x,t)}{D\tau} = -\frac{G(x,t)}{D} \quad (1)$$

Avec $D = D(\omega, kl, \phi)$ et,

$$D(\omega, kl, \phi) = D_0(kl, \phi) \left[\frac{1 + \omega^2 \tau^2}{(-\omega^2 \tau^2) + i\omega\tau} + \frac{-\omega^2 \tau^2 - 1}{(-\omega^2 \tau^2) + i\omega\tau} i \right]$$

$G(x,t)$ And $\delta(x,t)$ are respectively the global generation rate and the excess minority carriers density at position x and time t ; D is the diffusion coefficient; ω is the angular frequency; τ is minority carriers lifetime gotten from the empirical relation in term of the damage coefficient kl and the irradiation flux ϕ [3 ; 4],

$$\frac{1}{\tau} = \frac{1}{\tau_0} + kl.\phi \quad (2)$$

$G(x,t)$ and $\delta(x,t)$ can be written in the form as follows [5; 6]:

$$G(x,t) = g(x)e^{i\omega t} \text{ And } \delta(x,t) = \delta(x)e^{i\omega t} \quad (3)$$

Where, $g(x)$ and $\delta(x)$ typify the spatial components, $e^{i\omega t}$ the temporal component.

Inserting equation (3) in equation (1) and setting:

$$\frac{1}{L_\omega^2} = \frac{1}{L^2} (1 + i\omega\tau) \quad (4)$$

Where $L^2 = D(1 + i\omega\tau)$ with L being the complex diffusion length related to the irradiation energy and the damage coefficient by the following relation [7]:

$$L = L(kl, \phi) = \frac{1}{\sqrt{\frac{1}{L_0^2} + kl, \phi}} \quad (5)$$

We obtain:

$$\frac{\partial^2 \delta(x)}{\partial x^2} - \frac{\delta(x)}{L_\omega^2} = -\frac{g(x)}{D} \quad (6)$$

Where $g(x)$ and $L_\omega = L(kl, \phi)$ are given by:

$$L(kl, \phi) = L_0 \sqrt{\frac{1 - i\omega\tau}{1 + \phi\tau}} \quad (7)$$

$$g(x) = \alpha \cdot I_0 (1 - R) e^{-\alpha x} \quad (8)$$

$\alpha = \alpha(\lambda)$ and $R = R(\lambda)$ are respectively the monochromatic optical absorption coefficient and the cell monochromatic reflection coefficient at the wavelength λ ; H is the thickness of the solar cell.

The solution of the continuity equation is given by the following expression:

$$\delta(x) = A \cosh\left(\frac{x}{L_\omega}\right) + B \sinh\left(\frac{x}{L_\omega}\right) - \frac{\alpha I_0 (1 - R) L_\omega^2}{D(\alpha^2 L_\omega^2 - 1)} \exp(-\alpha x) \quad (9)$$

Where coefficient A and B are to be determined by use of the following boundary conditions [8, 9]:

- At the Junction ($x=0$)

$$\left. \frac{\partial \delta(x)}{\partial x} \right|_{x=0} = S f_j \cdot \frac{\delta(0)}{D} \quad (10)$$

- At the back surface ($x=H$)

$$\left. \frac{\partial \delta(x)}{\partial x} \right|_{x=H} = -S b_j \cdot \frac{\delta(H)}{D} \quad (11)$$

$S f_j$ and $S b_j$ are recombination velocity respectively at the junction and at the rear surface.

3. MINORITY CARRIERS DENSITY

The profile of the minority carriers density module versus particles Ennery is given in figure 2.

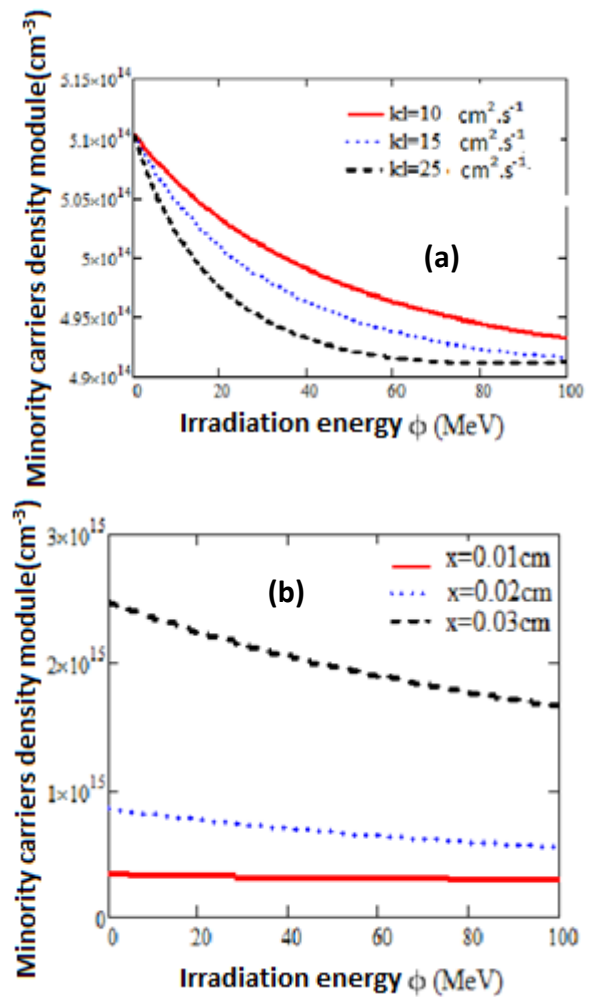


Figure 2: Minority carriers density Module versus irradiation energy for different values of the damage coefficient kl (a) and for different values of the depth (x) (b): $S b_j = S f_j = 3000 \text{ cm} \cdot \text{s}^{-1}$; $H = 0.03 \text{ cm}$; $\lambda = 0.98 \text{ } \mu\text{m}$; $Kl = 5 \text{ cm}^2/\text{s}$; $\omega = 10^3 \text{ rad/s}$.

On one hand both figure (a) and (b) show that minority carriers' density decreases with the increase of the irradiation flux. The concentration of carriers is maximal close to the junction. On the other hand, when the irradiation energy or the damage coefficient (expressing the faculty more or less big of a particle to cause some deteriorations within a material) increases, deteriorations are more significant for high damage coefficient values (a) and they are more noticeable in surface than in depth (b).

It seems that the important parameter here is the irradiation energy since significant decrease cannot be observed when irradiation energy is below a certain threshold.

4. PHOTOCOURANT DENSITY

The photocourant density is due to the minority charge carriers diffusion through the junction and it is given by the FICK law:

$$J(Sf_j, Sb_j, \lambda, \omega, kl, \phi) = q.D. \left. \frac{\partial \delta(x, Sf_j, Sb_j, \lambda, \omega, kl, \phi)}{\partial x} \right|_{x=0} \quad (12)$$

q is the elementary charge of electron and D is diffusion coefficient.

In figure 3 is represented the photocurrent density module versus the irradiation flux for various damage coefficient:

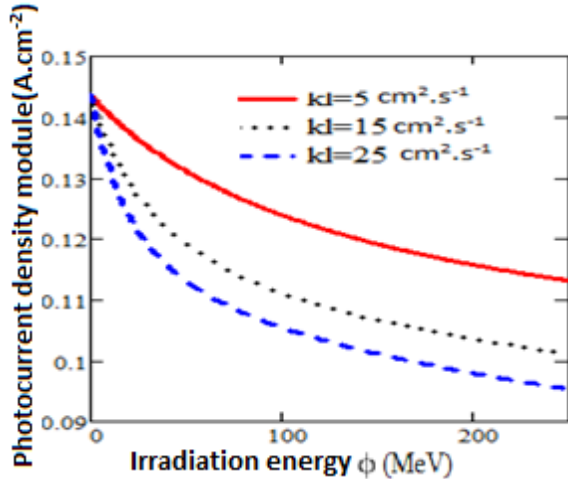


Figure 3: Photocurrent density module versus irradiation for various damage coefficient Kl : $Sb_j=2000 \text{ cm.s}^{-1}$; $Sf_j=410^4 \text{ cm.s}^{-11}$; $H=0.03 \text{ cm}$; $\lambda=0.78 \mu\text{m}$; $\omega=10^3 \text{ rad/s}$.

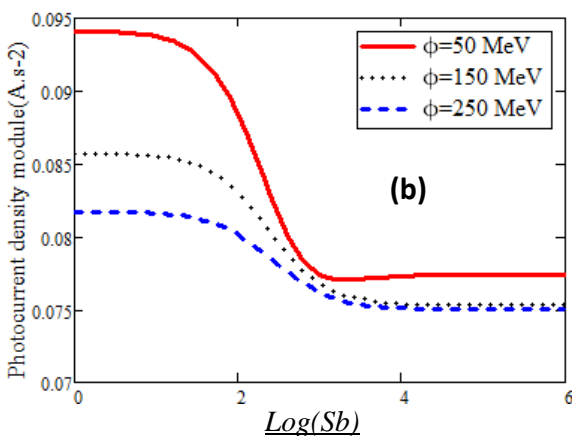
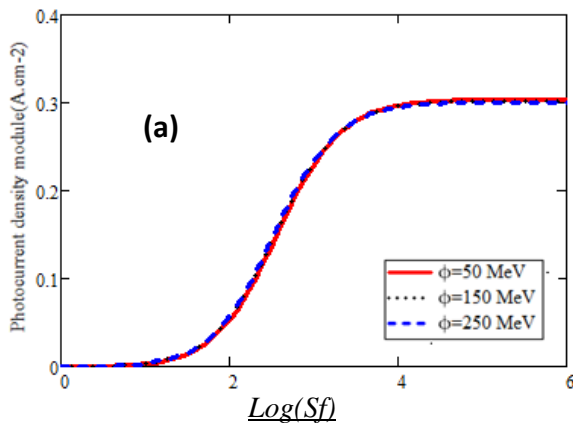


Figure4: Photocurrent density module versus recombination velocity Sf (a) and Sb (b) for various irradiation energy: $Sf_j=3.10^3 \text{ cm.s}^{-1}$; $H=0.03 \text{ cm}$; $\omega=10^4 \text{ rad/s}$; $\lambda=0.98 \mu\text{m}$

On figure 3 we note that the photocurrent density module decreases with the increase of the irradiation energy. Moreover, this decrease of the photocurrent density is more marked for high damage coefficient values.

The aspect of the curve on figure 4 shows that for low values of the recombination velocity at the junction, the photocurrent density module is nil. Then it increases with the recombination velocity Sf until a constant value giving the value of the short-circuit current. The curve on figure 5 gives the opposite effect. Indeed, the photocurrent density module is maximum for the lowest recombination values Sb corresponding to short-circuit current and is minimum to the highest recombination values Sb corresponding to open circuit current.

These graphs also point up the influence of the particles energy on the photocurrent density module. One observes that when particles energy increase, photocurrent density module decreases.

Indeed if the damage coefficient increases, the probability for a given energy to cause deteriorations will be high.

5. INTRINSIC RECOMBINATION VELOCITIES

The profile of photocurrent density in term of junction recombination velocity Sf_j and back surface recombination velocity Sb_m , present two stages. Thus, the expressions of the solar cell junction intrinsic recombination velocity Sf and back surface recombination velocity Sb are obtained below respectively from the equations (13) and (14).

$$\left. \frac{\partial J(Sf, Sb, \lambda, \omega, kl, \phi)}{\partial Sb_j} \right|_{Sb_j \rightarrow \infty} = 0 \quad (13)$$

$$\left. \frac{\partial J(Sf, Sb, \lambda, \omega, kl, \phi)}{\partial Sf_j} \right|_{Sf_j \rightarrow \infty} = 0 \quad (14)$$

$$S_x \mathcal{C}(\omega, kl, \phi) = \mathbf{F} \mathcal{C}(\omega, kl, \phi) + iG \mathcal{C}(\omega, kl, \phi)$$

The two expressions of the intrinsic recombination velocities are complex and therefore can be written as:

$$= |Sf \mathcal{C}(\omega, kl, \phi)| e^{i\phi_{sx}} \quad (15)$$

6. BODE AND NYQUIST DIAGRAM

The Nyquist diagram [10, 11, 12, 13] consists in representing the imaginary part of a physical magnitude versus its real part. Whereas Bode diagram [14] is a method developed to obtain the graph of the grandeur versus the frequency.

These two types of diagram are used to describe the electric recombination phenomena of the intrinsic

recombination velocities at the junction Sf and at the back surface Sb [15].

In the following graphs are plotted respectively the logarithm of the intrinsic recombination velocities module Sf and Sb and their phases versus the logarithm of the angular frequency for various irradiation energy (figure 5, 6, 7,8), and on figure 9 and 10 we have the imaginary part versus their real part for various irradiation energy.

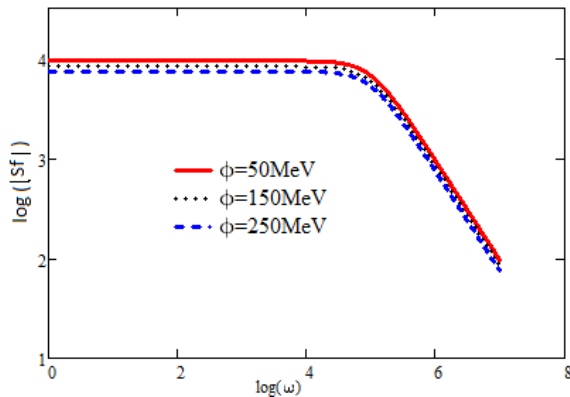


Figure 5: Logarithm of the module of Sf versus logarithm of ω . $\lambda=0.78 \mu\text{m}$; $kl=5\text{cm}^2/\text{s}$.

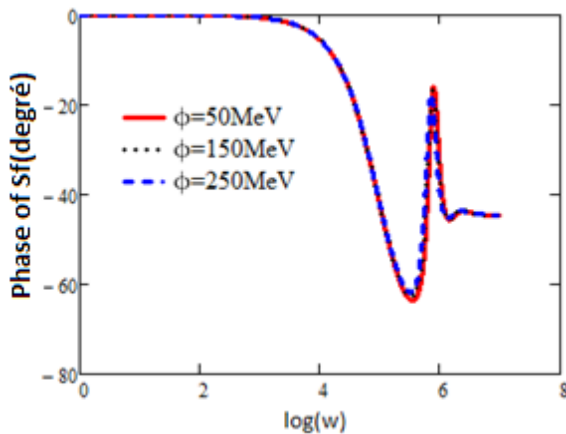


Figure 6: Phase of Sf versus the logarithm of ω ; $\lambda=0.94 \mu\text{m}$; $kl=5\text{cm}^2/\text{s}$.

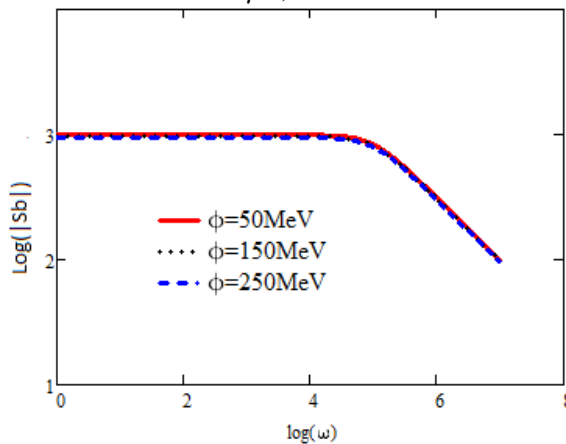


Figure 7: logarithm of the module of Sb versus logarithm of ω ; $\lambda=0.78 \mu\text{m}$; $kl=5\text{cm}^2/\text{s}$.

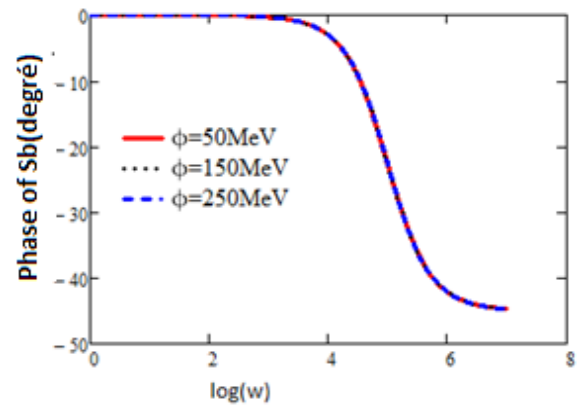


Figure 8: Phase of Sb versus logarithm of ω ; $\lambda=0.94 \mu\text{m}$; $kl=5\text{cm}^2/\text{s}$.

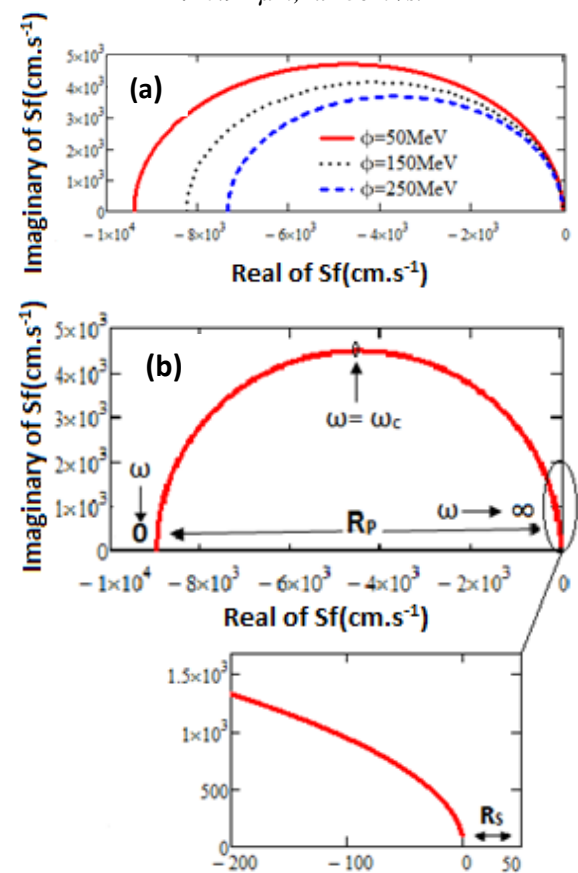
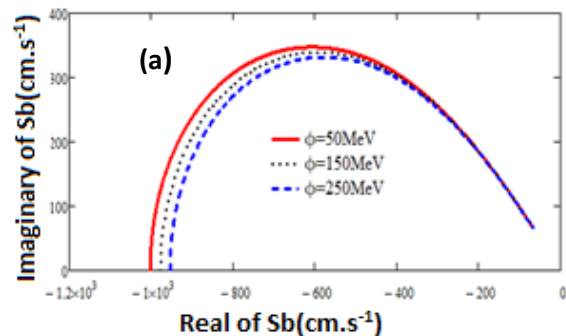


Figure 9: Imaginary part of Sf versus its real part;



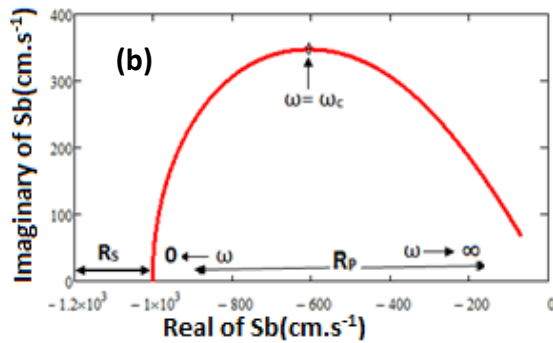


Figure 10: Imaginary part of S_b versus its real part ;
 $\lambda=0.78 \mu\text{m}$; $kl=5\text{cm}^2/\text{s}$.

In the angular frequency range $[0 \text{ rad.s}^{-1}, 10^4 \text{ rad.s}^{-1}]$, we are in quasi-static regime, means that $|S_f|$ and $|S_b|$ are independent of the frequency. But beyond 10^4 rad.s^{-1} $|S_f|$ and $|S_b|$ are steadily decreasing. Higher the energy, smaller the velocities become. Thus, irradiation and high frequency entail the slowing of electrons that move to the junction and increase their probability of recombination in the base, fig.5 and 7.

On fig. (9, a) and (10, a), we note that imaginary parts of S_f and S_b are positive but real parts are negative. Gotten curves are in the form of semi-circles with variable diameters according to the energy (small energy values give large diameters). Figures (6) and (8) show that the phase is always negative. Therefore, capacitive effects prevail against inductive effects.

Fig. (9, b) and (10, b) illustrate three characteristic points corresponding to angular frequency: $\omega = 0$, $\omega = \omega_c$ and $\omega \rightarrow \infty$. At $\omega = 0$, the imaginary part is nil while the real part corresponds to a value different from zero. When $\omega = \omega_c$, the imaginary part is maximal but both imaginary and real parts are different from zero.

The minority carrier's diffusion begins to decrease since there is rupture of generation. When $\omega \rightarrow \infty$, both imaginary and real parts are nil. What allows us to determine the diameter of the semi-circle.

Based on the interpretations of Bode and Nyquist diagrams, an equivalent circuit describing the electric behavior of the cell is represented in the following figure:

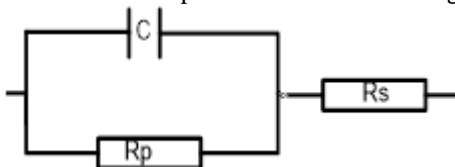


Figure 11: equivalent electric model

Where C is a capacitance of a capacitor describing the capacitive recombination velocity; R_p is a parallel resistance and R_s is a series resistance

Nyquist diagram provides us the diameter of the semi-circle which is equal to R_p [16, 17] Knowing the value of cut-off frequency ω_c , we can deduce the minority carriers

lifetime photo generated and the capacitance from the relation $\tau = 1/\omega_c$ and $\tau = R_p \cdot C$ [18].

7. CONCLUSION

Bifacial solar cell study showed us that its parameters depend strongly on the irradiation energy and the damage coefficient. The negative influence of irradiation particles is more accentuated for the high energy values. So it's clear that even with low energy values, for a long exhibition to the irradiations, the effects will be considerable.

REFERENCES

- [1] **Hübner, A., Aberle, A.G. and Hezel, R.** (2001) 20% Efficient Bifacial Silicon Solar Cells. 14th European Photovoltaic Solar Energy Conference, Munich, 2001, 1796-1798.
- [2] **Meier, D.L., Hwang, J.-M. and Campbell, R.B.** (1988) The Effect of Doping Density and Injection Level on Minority-Carrier Lifetime as Applied to Bifacial Dendritic Web Silicon Solar Cells. IEEE Transactions on Electron Devices, **ED-35**, 70-78.
- [3] **M.A. Ould El Moujtaba, M. Ndiaye, A.Diao, M.Thiame, I.F. Barro and G. Sissoko.** Theoretical Study of the Influence of Irradiation on a Silicon Solar Cell under Multispectral Illumination. Res. J. Appl. Sci. Eng. Technol., 4(23): 5068-5073, 2012
- [4] **I.Ly, M.Wade, H.Ly Diallo, M.A.El Moujtaba, O.H.Lemrabott, S.Mbodj, O.Diasse, A.Ndiaye, I.Gueye, F.I.Barro, A.Wareme, G.Sissoko.** Irradiation Effect on the Electrical Parameters of a Bifacial Silicon Solar Cell under Multispectral Illumination : 26ème Conférence Européenne sur l'Energie Solaire Photovoltaïque (26th EU PVSEC), 785-788.
- [5] **Andreas Mandelis** J. Appl. Phys. Vol.66 N°11, 1 December 1989, pp 5572583
- [6] **J.N. Hollenhorst and G. Hasnain** Appl. Phys. Lett. Vol.67(15), (1995), pp 2203-2205
- [7] **Kraner, H.W.**, 1983. Radiation damage in silicon detectors. 2nd Pisa Meeting on Advanced Detectors, Grosseto, Italy, June 3-7.
- [8] **G.Sissoko, C. Museruka, A. Corr ea, I. Gaye, A. L.Ndiaye.** World Renewable Energy Congress (1996), part III, pp.1487-1490
- [9] **H.L. Diallo, A. Seidou Maiga, A. Wereme, and G.Sissoko.** "New approach of both junction and back surface recombination velocities in a 3D modelling study of a polycrystalline silicon solar cell" Eur. Phys. J. Appl. Phys. 42, 203–211 (2008)
- [10] **R. Anil Kumar, M.S. Suresh and J. Nagaraju .** Measurement of AC parameters of Gallium Arsenide (GaAs/Ge) solar cell by impedance spectroscopy. IEEE Transactions on Electron Devices, Vol.48, No.9, September 2001.

- [11] **D. Chenvidhya, K. Kirikara, C. Jivacate** A new characterization method for solar cell dynamic impedance, solar energy materials and solar cells 80 (2003) 459-465. Solar Energy Materials and Solar Cells 86 (2005) 243-251
- [12] **I. Gaye, A. Correa, B. Ba, A. L. Ndiaye, E. Nanema, A. B. B. Ba, M. Adj And G. Sissoko.** Impedance parameters determination of silicon solar cell using the one diode model in transient
- [13] **D. Chenvidhya, K. Kirtikara, C. Jivacate,** "A new characterization method for solar cell dynamic impedance," Solar Energy Materials and Solar Cells, Vol.80, No.4, 2003, pp.459-464
- [14] Lathi, Bhagwandas Pannalal: Signals, Systems and Controls. Intext Educational Publisher, New York, 1973-1974. study, Renewable Energy, Vol 3, pp1598-1601,1996.
- [15] **Nd Thiam, A. Diao, M. Ndiaye, A. Dieng, A. Thiam, M. Sarr, A.S. Maiga And G. Sissoko,** "Electric equivalent models of intrinsic recombination velocities of a bifacial silicon solar cell under frequency modulation and magnetic field effect," Research Journal of Applied Sciences, Engineering and Technology, Vol.4, No.22, 2012, pp.4646-4655
- [16] **M. S. Suresh,** "Measurement of solar cell parameters using impedance spectroscopy," Solar Energy Materials and Solar Cells, Vol.43, Issue1, 1996, pp.21-28
- [17] **R. A. Kumar, M. S. Suresh, J. Nagaraju,** "Measurement of AC parameters for Gallium Arsenide (GaAs/Ge) solar cell by impedance spectroscopy," IEEE Transactions on Electron Devices. Vol.48, No.9, 2001, pp.2177-2179
- [18] **M. Ndiaye, Z. Nouhou Bako, I. Zerbo, A. Dieng, F. I. Barro, G. Sissoko,** "détermination des paramètres électriques d'une photopile sous éclairage monochromatique en modulation de fréquence, à partir des diagrammes de bode et de nyquist," / J. Sci. Vol. 8, N° 3 (2008) pp59-68.
- [19] **G., Sissoko, E. Nanéma, A. Corrèa, P. M. Bitèye, M. Adj and A.L. N'Diaye,** 1998. Silicon solar cell recombination parameters determination using the illuminated I-V characteristic. World Renewable Energy Congress, pp : 1847-1851.
- [20] **F.I. Barro, S. Mbodji ; A.L. N'Diaye, I. Zerbo, S. Madougou, F. Zougmore and G. Sissoko,** 2004. Bulk and surface parameters determination by a transient study of a bifacial silicon solar cell under constant white bias light. Proceedings of the 19th European Photovoltaic Solar Energy Conference and Exhibition, pp : 262-265.
- [21] **H.L. Diallo, A.S. Maiga, A. Wereme and G. Sissoko,** 2008. New approach of both junction and back surface recombination velocities in a 3D modeling study of a polycrystalline silicon solar cell. Eur. Phys. J. Appl. Phys., 42 : 203-211.